Two-input two-output port model for mechanical systems

D. Alazard [*], J. Alvaro Perez, [†]T. Loquen, C. Cumer [‡]

This paper proposes a double input output port transfer to model complex mechanical systems composed of several sub-systems. The sub-structure decomposition is revisited from the control designer point of view. The objective is to develop modelling tools to be used for mechanical/control co-design of large space flexible structures involving various substructures (boom, links of robotic arm,...) connected one to each other through dynamics local (actuated) mechanisms inducing complex boundary conditions. The double input output port model of each substructure is a transfer where accelerations and external forces at the connection points are both on the model inputs and outputs. Such a model :

- **allows to the boundary conditions linked to interactions with the other substructures to be externalized outside the model,**
- **is defined by the only substructure own dynamic parameters,**
- **allows to build the dynamic model of the whole structure by just assembling the double port models of each substructure.**

The principle is first introduced on a single axis spring-mass system and then extented to the 6 degress-of-freedom case. This generalization uses the clamped-free substructure dynamic parameters such as finite element softwares can provide.

Nomenclature

General notations:

$[X]_{\mathcal{R}}$	:	model, vector or matrix X projected in the frame $\mathcal{R}$.
$\frac{d\overrightarrow{X}}{dt}\|_{\mathcal{R}} = 0$	:	time-derivation of the vector $\overrightarrow{X}$ w.r.t the frame $\mathcal{R}$.
$\vec{u} \wedge \vec{v}$	:	cross product of vectors $\vec{u}$ and $\vec{v}$ ($\vec{u} \wedge \vec{v} = (^*\vec{u})\vec{v}$)
$\vec{u}.\vec{v}$	:	dot product $\vec{u}$ and $\vec{v}$ ($\vec{u}.\vec{v} = [\vec{u}]_{\mathcal{R}}^T [\vec{v}]_{\mathcal{R}}$, $\forall \mathcal{R}$)
$\mathbf{s}$	:	Laplace variable.
I_n	:	Identity matrix $n \times n$.
$0_{n\times m}$	:	null matrix $n \times m$.
A^T	:	A transposed.
$\text{diag}(\omega_i)$	:	diagonal matrix $N \times N$: $\text{diag}(\omega_i)(i,i) = \omega_i$, $i = 1, \cdots, N$.
$P(\mathbf{s})(i:j, l:m)$	:	subsystem of $P(\mathbf{s})$ restricted to inputs l to m and to inputs i to j.

See also Figure 14 for the following notations:

$\mathcal{A}$	:	the substructure (or body) considered for the modeling.
$\mathcal{P}$	:	the parent substructure (or body) of $\mathcal{A}$.
$\mathcal{C}$	:	the child substructure (or body) of $\mathcal{A}$.

[*]Professor, University of Toulouse-ISAE, 10, Av. Edouard Belin, Toulouse- 31055 FRANCE. (Email: daniel.alazard@isae.fr)
[†]PhD. University of Toulouse-ISAE, 10, Av. Edouard Belin, Toulouse- 31055 FRANCE
[‡]Research Scientists, ONERA, 2, Av. Edouard Belin, Toulouse- 31055 FRANCE.

$\mathcal{R}_a = (P, \vec{x}_a, \vec{y}_a, \vec{z}_a)$	:	body $\mathcal{A}$ reference frame, where P denotes the anchorage point between $\mathcal{A}$ and $\mathcal{P}$. $\vec{x}_a$, $\vec{y}_a$, $\vec{z}_a$ are unitary vectors.
A	:	centre of mass of body $\mathcal{A}$.
$\overrightarrow{a}_P$	:	absolute linear acceleration vector of point P.
$\overrightarrow{\omega}_P$	:	absolute angular velocity vector of point P.
$\ddot{\mathrm{x}}_P$	:	dual (6 components) vector of accelerations at point P.
$\overrightarrow{F}_{\mathcal{A}/\mathcal{P}}$	:	interaction force by $\mathcal{A}$ on $\mathcal{P}$.
$\overrightarrow{T}_{\mathcal{A}/\mathcal{P},P}$	:	interaction torque by $\mathcal{A}$ on $\mathcal{P}$ at point P.
$\mathrm{F}_{\mathcal{A}/\mathcal{P},P}$	:	dual (6 components) vector of interactions at point P.
$\overrightarrow{a}_C$	:	absolute linear acceleration vector of point C.
$\overrightarrow{\omega}_C$	:	absolute angular velocity vector of point C.
$\ddot{\mathrm{x}}_C$	:	dual (6 components) vector of accelerations at point C.
$\overrightarrow{F}_{\mathcal{C}/\mathcal{A}}$	:	interaction force by $\mathcal{C}$ on $\mathcal{A}$.
$\overrightarrow{T}_{\mathcal{C}/\mathcal{A},C}$	:	interaction torque by $\mathcal{C}$ on $\mathcal{A}$ at point C.
$\mathrm{F}_{\mathcal{A}/\mathcal{P},C}$	:	dual (6 components) vector of interactions at point C.
$M_P^{\mathcal{A}}(\mathrm{s})$	:	direct dynamic model of the body $\mathcal{A}$ at point P.
$m^{\mathcal{A}}$	:	mass of body $\mathcal{A}$.
$\mathbb{I}_A^{\mathcal{A}}$	:	moment of inertia tensor of body $\mathcal{A}$ at the point A.
τ_{CP}	:	kinematic model between the point C and the point P: $\tau_{CP} = \begin{bmatrix} I_3 & (^*\overrightarrow{CP}) \\ 0_{3\times 3} & I_3 \end{bmatrix}$.
$(^*\overrightarrow{CP})$	:	antisymmetric matrix associated to the vector $\overrightarrow{CP}$: if $\overrightarrow{CP} = \begin{bmatrix} x \\ y \\ z \end{bmatrix}_{\mathcal{R}}$ then $\left[(^*\overrightarrow{PB})\right]_{\mathcal{R}} = \begin{bmatrix} 0 & -z & y \\ z & 0 & -x \\ -y & x & 0 \end{bmatrix}_{\mathcal{R}}$ $\forall\, \mathcal{R}$.
N_m	:	number of mesh nodes.
P_i	:	$(i = 1, \cdots, N_m)$ nodes of the meshing.
q	:	$(6\,N_m \times 1)$ vector of degrees-of-freedom.
$\delta\mathrm{x}_C$	:	(6×1) vector of the 6 displacements of the node C in $\mathcal{R}_a$.
$\delta\mathrm{x}_{\neq C}$	:	$(6\,(N_m - 1) \times 1)$ vector of displacements at the other nodes $P_i \neq C$.
N	:	number of flexible modes ($N = 6N_m$).
η	:	vector of modal coordinates.
ω_i	:	frequency of the i^{th} flexible mode.
ξ_i	:	modal damping ratio if the i^{th} flexible mode.
$l_{i,P}$	:	1×6 modal participation factor of the i^{th} flexible mode flexible at point P.
L_P	:	matrix $N \times 6$ of modal participation factors at point P ($L_P = [l_{1,P}^T,\ l_{2,P}^T, \cdots,\ l_{N,P}^T]^T$).
Φ	:	$(N \times N)$ modal shape matrix.
Φ_C	:	$(6 \times N)$ projection of the n modal shapes on the 6 d.o.f $\delta\mathrm{x}_C$ ($\Phi_C = \Phi(1:6,:)$).
$\Phi_{\neq C}$	:	$((N-6) \times N)$ projection of the n modal shapes on the other d.o.f.
$\vec{r}_a$	:	unit vector along the revolute joint axis (if present): $\vec{r}_a = [x_{r_a}\ y_{r_a}\ z_{r_a}]_{\mathcal{R}_a}^T$.

I. Introduction

Space system engineering requires some tools to manage main trade-off as soon as possible in the spacecraft design process. The classical process where the control engineer has to design a control law meeting some specifications for a given mechanical and avionics architecture can bring some time-consuming iterations with the overall system designer. Designing main mechanical parameters, main avionics characteristics and the associated control law in one shot could save lots of time. Today some tools are available to optimize the parameters of a fixed-structure control system and it seems interesting to include in the set of decision variables some parameters characterizing the mechanical or avionics design. In,[1] some methods and tools were proposed for control/avionics co-design. The model was based on previous developments[2] to build the overall model of the spacecraft composed of a main body and various flexible appendages connected to the main body through clamped or revolute joints. Such a method is restricted to open-chain mechanical systems where flexible bodies are the ending bodies (leaves) of the various chains (or branches). Indeed, any open-chain mechanical system can be describe by a tree where each node corresponds to a body (or substructure) and each edge corresponds to a joint between two bodies. Thus, classical tree terminology will be used in this paper (root, leaf, parent, child).

In the scope to perform mechanical/control co-design, for instance for sizing the main mechanical parameters of a space robotics arms and for designing the control laws to meet some specifications (bandwitdh, accuracy) at the end-effector level, some modelling tools are still required to model arbitrary open-chain mechanical systems composed of flexible bodies. Such a model must be able to be augmented with the model of local mechanisms (actuator, gear stiffness,...) lumped at the connecting points between the various substructures or bodies. These mechanisms induce complex boundary conditions (between free and clamped boundary conditions) which are more determinant on the dynamic behavior of the overall system than a too rich (and too high order) representation of the internal flexible modes of the each substructure.

With this scope in mind, the proposed approach aims to develop a double input output port transfer to model each substructure. This double input output port model is a multi-input multi-output transfer with two channels. The first one represents the inverse dynamic model (forces on input and accelerations on output) at the connecting point between the substructure and the child structure. The second channel represents the direct dynamic model (accelerations on input and forces on output) at the connecting point between the substructure and parent structure. The state-space representation of the double-port model is minimal such that there is no extra state variables to represent the direct and the inverse dynamic models. There are some strong links between this approach and the Graig-Bampton substructure coupling approach[3,4] more generally known in the field of finite element method applied to structure dynamics. Taking into account that, for the considered space applications, the boundary degrees-of-freedom of the Graig-Bampton approach are reduced to the 6 degrees-of-freedoom (3 translations and 3 rotations) of the connection point, one can externalize the accelerations and external forces at this point to plug any kind of boundary conditions (free, clamped, or more complex boundary conditions provided by a dynamic local mechanism). There are also some links with the port-hamiltonian representation of complex physical systems involving interconnected sub-systems, lumped or distributed parameters.[5–7]

In the first section, an introductive single-axis example is presented to highlifht the basic principle.

In the second section the generalization to the 6 degrees of freedom case for any kinds of mechanical substructure is derived from the output data commonly provided by F.E (Finite Elements) softwares (i.e.: pulsations, damping ratios, modal participation factors, and modal shapes of the substructure) and commonly used in space engineering.

II. An introductive example

The objective is to model any kind of **open-chain** mechanical systems composed of spring-mass subsystems all working along the same axis $\overrightarrow{x}$. An example of such a system is depicted in Figure 1.

Mechanical engineers often debate the question:
Who, between the force $\overrightarrow{f}$ and the acceleration $\overrightarrow{\gamma}$, is the cause or the effect in the well-known relationship $\overrightarrow{f} = m\overrightarrow{\gamma}$?.
The two port approach will put anyone agree !!: a double port dynamic model $Z_i(\mathbf{s})$ is developped to represent the elementary spring-mass system presented in Figure 3. The block-diagram representation of this dynamic

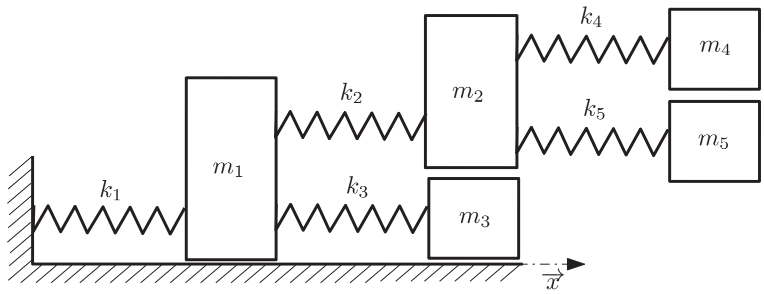

Figure 1. An open-chain mechanical system composed of 5 spring-mass subsystems.

model (also called quadripole [a] because it is a 2×2 transfer) is presented in Figure 2 and highlights that acceleration and force are both on the inputs or the outputs of $Z_i(\mathbf{s})$:

$$\begin{bmatrix} \ddot{X}_i(\mathbf{s}) \\ F_{i/i-1}(\mathbf{s}) \end{bmatrix} = Z_i(\mathbf{s}) \begin{bmatrix} F_{i+1/i}(\mathbf{s}) \\ \ddot{X}_{i-1}(\mathbf{s}) \end{bmatrix}$$

- $F_{i/i-1}(\mathbf{s}) = \mathcal{L}[f_{i/i-1}(t)]$ is the force applied by the i-th spring-mass system on the parent [b] (or left-hand side) substructure ($X(\mathbf{s}) = \mathcal{L}[x(t)]$ is the LAPLACE transform of $x(t)$),
- $F_{i+1/i}(\mathbf{s}) = \mathcal{L}[f_{i+1/i}(t)]$ is the force applied by the child (or right-hand side) sub-structure on the i-th spring-mass system,
- $\ddot{X}_{i-1}(\mathbf{s}) = \mathcal{L}[\ddot{x}_{i-1}(t)]$ is the inertial acceleration of the connecting point (interface) between i-th spring-mass system and the parent substructure,
- $\ddot{X}_i(\mathbf{s}) = \mathcal{L}[\ddot{x}_i(t)]$ is the inertial acceleration of the connecting point between i-th spring-mass system and the child substructure.

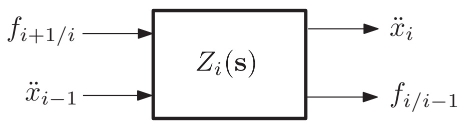

Figure 2. Double port dynamic model $Z_i(\mathbf{s})$ of the elementary spring mass system.

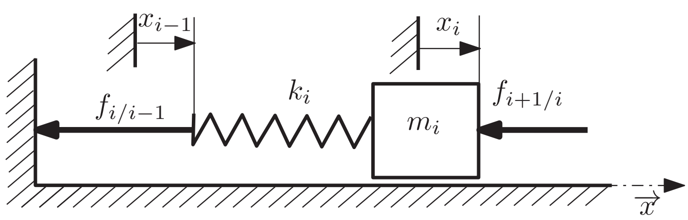

Figure 3. The elementary spring-mass system.

From the NEWTON principle, one can easily derive the following equations that govern the dynamical behavior of the elementary spring-mass system:

$$m_i \ddot{x}_i = f_{i+1/i} - f_{i/i-1} \quad (1)$$

$$f_{i/i-1} = k_i(x_i - x_{i-1}) \, . \quad (2)$$

These equations can be represented by the block diagram depicted in Figure 4.

[a] Indeed, there is a link with quadripoles or impedance models used in electrical engineering or in mechanical engineering but the particularity of this double-port model is that it considers accelerations instead of velocities.

[b] In this context, the parent sense is towards the inertial and fixed frame.

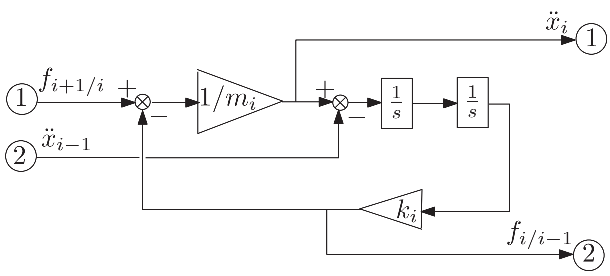

Figure 4. Block-diagram représentation of $Z_i(\mathbf{s})$.

Thus, $Z_i(\mathbf{s})$ is a second order transfer and can be represented by:

- the state space representation associated to the state $x = [\delta x_i \quad \dot{\delta x}_i]^T$ with $\delta x_i = x_i - x_{i-1}$ (i.e.: the outputs of integrators in Figure 4):

$$\left[\begin{array}{c} \dot{\delta x}_i \\ \ddot{\delta x}_i \\ \hline \ddot{x}_i \\ f_{i/i-1} \end{array}\right] = \left[\begin{array}{cc|cc} 0 & 1 & 0 & 0 \\ -k_i/m_i & 0 & 1/m_i & -1 \\ \hline -k_i/m_i & 0 & 1/m_i & 0 \\ k_i & 0 & 0 & 0 \end{array}\right] \left[\begin{array}{c} \delta x_i \\ \dot{\delta x}_i \\ \hline f_{i+1/i} \\ \ddot{x}_{i-1} \end{array}\right]. \quad (3)$$

- the matrix of transfers:

$$Z_i(\mathbf{s}) = \frac{\left[\begin{array}{cc} \mathbf{s}^2 & k_i \\ k_i & -m_i k_i \end{array}\right]}{m_i \mathbf{s}^2 + k_i}. \quad (4)$$

The upper channel of $Z_i(\mathbf{s})$ (from $f_{i+1/i}$ to $\ddot{x}_i$) is homegeneous to a **inverse** dynamic model and can be expressed in Kg^{-1} and the lower channel of $Z_i(\mathbf{s})$ (from $\ddot{x}_{i-1}$ to $f_{i/i-1}$) is homegeneous to a **direct** dynamic model and can be expressed in Kg.

From the block diagram depicted in Figure 4, one can create a subsystem block $Z_i(\mathbf{s})$ completely characterized by the 2 dynamical parameters m_i and k_i (see Figure 5).

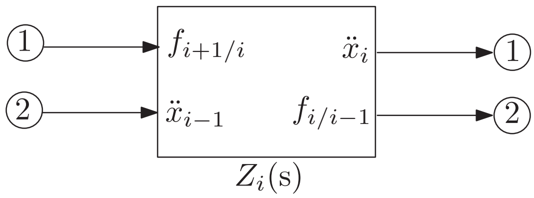

Figure 5. The subsystem $Z_i(\mathbf{s})$.

Then, the model of the example presented in Figure 1 can be directly described by a block diagram (see Figure 6) involving 5 blocks Z_i, $i = 1, \cdots, 5$ and the interactions between these 5 blocks are directly translated by lines between the blocks. These interactions are in fact the constraints or boundary conditions on the inputs of the Z_i blocks which are summarized in Table 1 (left).

One can also defined some inputs and ouputs for the whole system. For instance, Figure 7 represents the same system with an actuated force u between masses 1 and 2. The boundary conditions are then displayed in Table 1 (right) and the transfer between u and the position x_3 of the third mass can be described by the block diagram presented in Figure 8.

Now we consider the classical 2 masses + 1 string system depicted in Figure 9.

The objective is now to compute the new elementary transfer, noted $\mathcal{Z}(\mathbf{s}, m_{i-1}, k_i, m_i)$ between $f_{i+1/i}$, $\ddot{x}_{i-1}$ on the inputs and x_i, $f_{i/i-1}$ on the outputs. The definition of these variables is the same than in the previous case and it can be noticed that the transfer $Z_i(\mathbf{s})$ defined for the elementary spring-mass system

i	$f_{i+1/i}$	$\ddot{x}_{i-1}$
1	$f_{2/1} + f_{3/1}$	0
2	$f_{4/2} + f_{5/2}$	$\ddot{x}_1$
3	0	$\ddot{x}_1$
4	0	$\ddot{x}_2$
5	0	$\ddot{x}_2$

i	$f_{i+1/i}$	$\ddot{x}_{i-1}$
1	$f_{2/1} + f_{3/1} - u$	0
2	$f_{4/2} + f_{5/2} + u$	$\ddot{x}_1$
3	0	$\ddot{x}_1$
4	0	$\ddot{x}_2$
5	0	$\ddot{x}_2$

Table 1. Boundary conditions on the 5 blocks Z_i for the examples of Figure 1 (left) and Figure 7 (right).

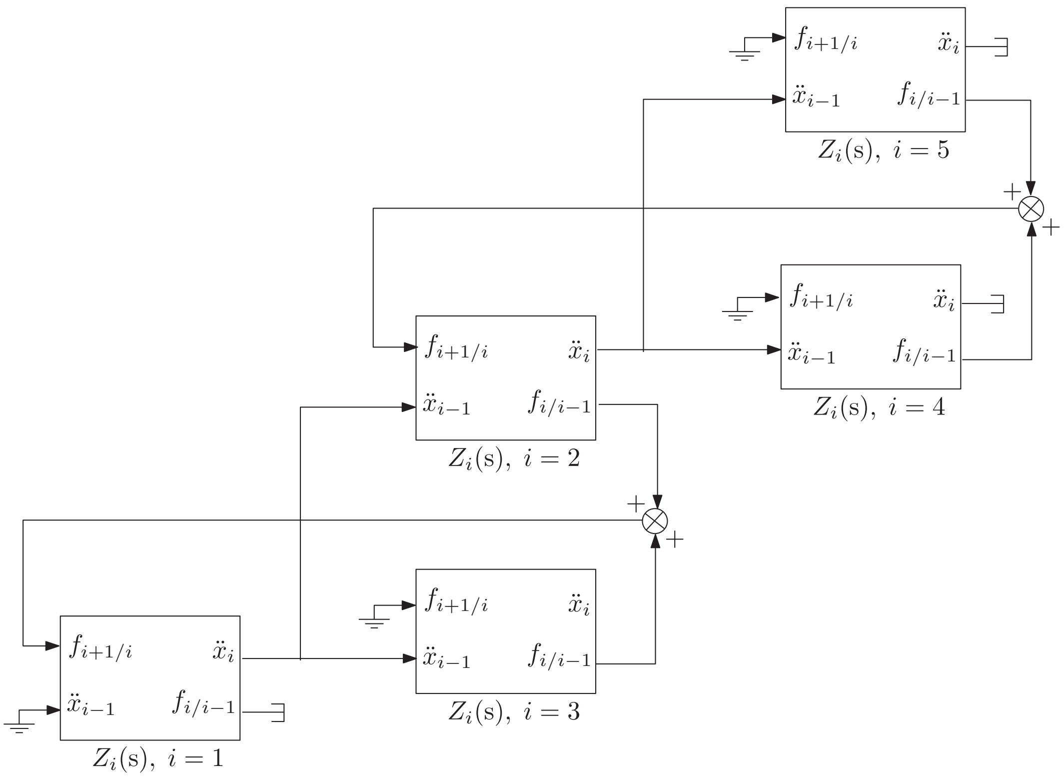

Figure 6. Block diagram corresponding to the example of Figure 1.

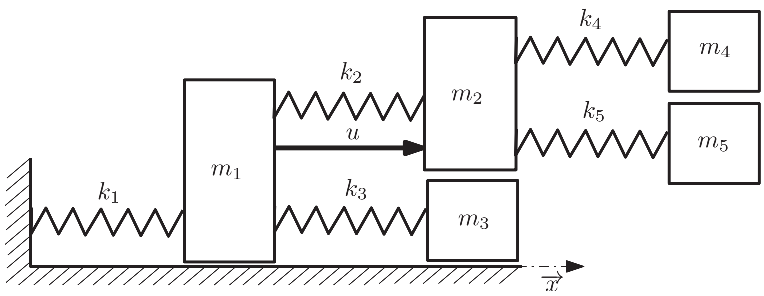

Figure 7. An open-chain mechanical system composed of 5 spring-mass systems with a force actuator between masses 1 and 2.

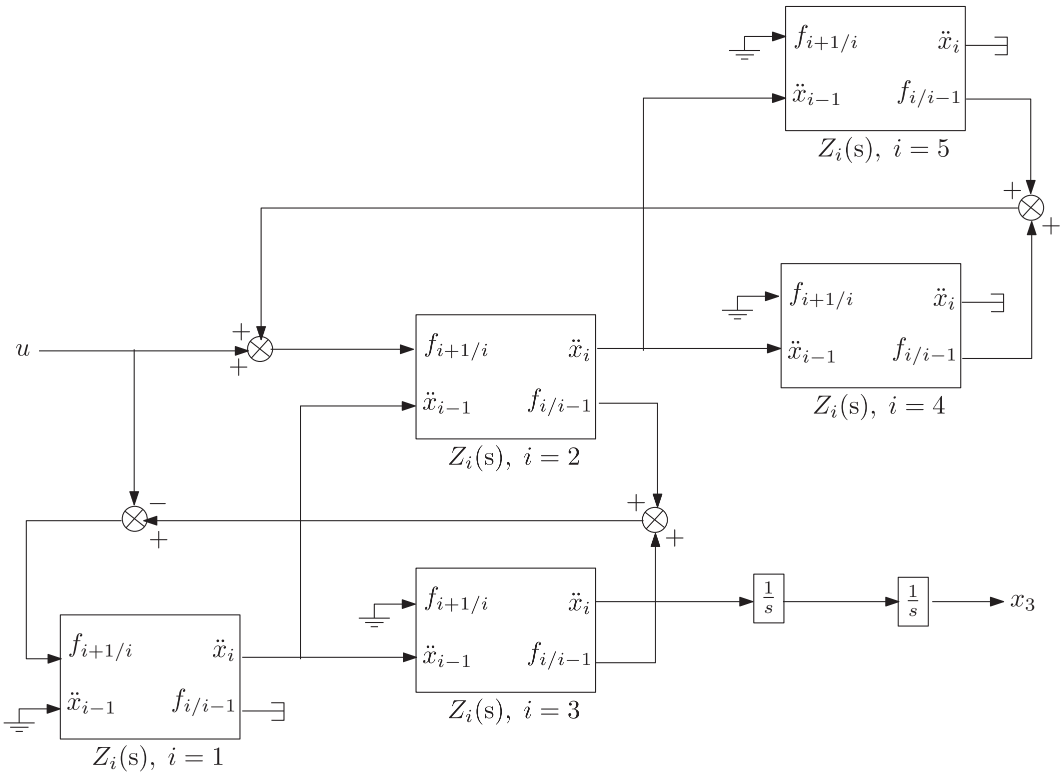

Figure 8. The block-diagram corresponding to the example of Figure 7.

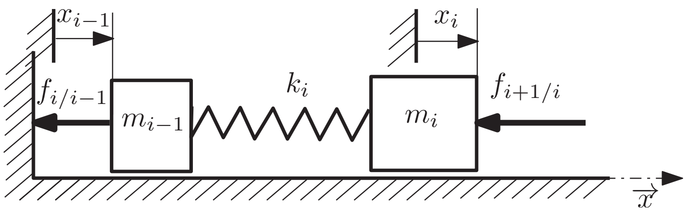

Figure 9. The spring mass system.

(Figure 3) reads $Z_i(\mathbf{s}) = \mathcal{Z}(\mathbf{s}, 0, k_i, m_i)$. From NEWTON principle applied to the mass m_{i-1}, the new transfer $\mathcal{Z}(\mathbf{s}, m_{i-1}, k_i, m_i)$ can be described by the block diagram depicted in Figure 10 and represented by:

- the state space representation associated to the state $x = [\delta x_i \quad \dot{\delta x_i}]^T$ with $\delta x_i = x_i - x_{i-1}$:

$$\boxed{\left[\begin{array}{c} \dot{\delta x_i} \\ \ddot{\delta x_i} \\ \hline \ddot{x}_i \\ f_{i/i-1} \end{array}\right] = \left[\begin{array}{cc|cc} 0 & 1 & 0 & 0 \\ -k_i/m_i & 0 & 1/m_i & -1 \\ \hline -k_i/m_i & 0 & 1/m_i & 0 \\ k_i & 0 & 0 & -m_{i-1} \end{array}\right] \left[\begin{array}{c} \delta x_i \\ \dot{\delta x_i} \\ \hline f_{i+1/i} \\ \ddot{x}_{i-1} \end{array}\right]} \tag{5}$$

- the matrix of transfers:

$$\boxed{\mathcal{Z}(\mathbf{s}, m_{i-1}, k_i, m_i) = \frac{\left[\begin{array}{cc} \mathbf{s}^2 & k_i \\ k_i & -m_i m_{i-1}(\mathbf{s}^2 + \omega_f^2) \end{array}\right]}{m_i(\mathbf{s}^2 + \omega_{c,p}^2)}} \,. \tag{6}$$

  where $\omega_f = \sqrt{\frac{k_i(m_{i-1}+m_i)}{m_{i-1}m_i}}$ is the free pulsation of the spring-mass system and $\omega_{c,p} = \sqrt{\frac{k_i}{m_i}}$ is the "parent cantilevered" frequency (that is, when the mass m_{i-1} is clamped on the inertial frame),

- the port-Hamiltoian representation, involving the "free" hamiltonian function $H = \frac{1}{2}m_i\dot{\delta x}_i^2 + \frac{1}{2}k_i\delta x_i^2$ (i.e.: the sum of kinematic and potential energies when inputs $f_{i+1/i}$ and $\ddot{x}_{i-1}$ are null):

$$\begin{array}{l} \left\{\begin{array}{lcl} \dot{q} & = & \frac{\partial H}{\partial p} \\ \dot{p} & = & -\frac{\partial H}{\partial q} + [1 \quad -m_i]\left[\begin{array}{c} f_{i+1/i} \\ \ddot{x}_{i-1} \end{array}\right] \end{array}\right. \\ \left[\begin{array}{c} \ddot{x}_i \\ f_i \end{array}\right] = \left[\begin{array}{c} \frac{1}{m_i} \\ -1 \end{array}\right]\dot{p} + \left[\begin{array}{cc} 0 & 1 \\ 1 & -(m_{i-1}+m_i) \end{array}\right]\left[\begin{array}{c} f_{i+1/i} \\ \ddot{x}_{i-1} \end{array}\right] \end{array} \tag{7}$$

  where $q = \delta x_i$ and $p = m_i\,\dot{\delta x_i}$.

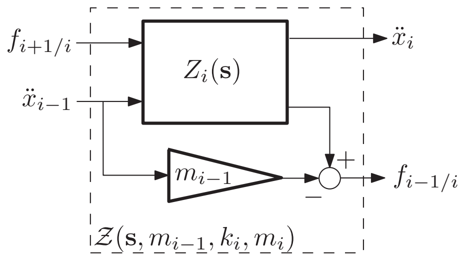

Figure 10. Double port model $\mathcal{Z}(\mathbf{s}, m_{i-1}, k_i, m_i)$ of the spring-mass system.

The main interest of $\mathcal{Z}(\mathbf{s}, m_{i-1}, k_i, m_i)$ w.r.t. $Z_i(\mathbf{s})$ is that it is invertible:

$$\mathcal{Z}^{-1}(\mathbf{s}, m_{i-1}, k_i, m_i) \;/\; \left[\begin{array}{c} \dot{\delta x_i} \\ \ddot{\delta x_i} \\ \hline f_{i+1/i} \\ \ddot{x}_{i-1} \end{array}\right] = \left[\begin{array}{cc|cc} 0 & 1 & 0 & 0 \\ -k_i/m_{i-1} & 0 & 1 & 1/m_{i-1} \\ \hline k_i & 0 & m_i & 0 \\ k_i/m_{i-1} & 0 & 0 & -1/m_{i-1} \end{array}\right] \left[\begin{array}{c} \delta x_i \\ \dot{\delta x_i} \\ \hline \ddot{x}_i \\ f_{i/i_1} \end{array}\right]$$

The upper channel is also invertible. Let $\mathcal{Z}^{-1^u}$, the operation corresponding to the inversion of the upper channel of $\mathcal{Z}$ only:

$$\mathcal{Z}^{-1^u}(\mathbf{s}, m_{i-1}, k_i, m_i) \;/\; \left[\begin{array}{c} \dot{\delta x_i} \\ \ddot{\delta x_i} \\ \hline f_{i+1/i} \\ f_{i/i-1} \end{array}\right] = \left[\begin{array}{cc|cc} 0 & 1 & 0 & 0 \\ 0 & 0 & 1 & -1 \\ \hline k_i & 0 & m_i & 0 \\ k_i & 0 & 0 & -m_{i-1} \end{array}\right] \left[\begin{array}{c} \delta x_i \\ \dot{\delta x_i} \\ \hline \ddot{x}_i \\ \ddot{x}_{i-1} \end{array}\right] .$$

The lower channel is also invertible. Let $\mathcal{Z}^{-1_l}$, the operation corresponding to the inversion of the lower channel of $\mathcal{Z}$ only:

$$\mathcal{Z}^{-1_l}(\mathbf{s}, m_{i-1}, k_i, m_i) \;/\; \left[\begin{array}{c} \dot{\delta x_i} \\ \ddot{\delta x_i} \\ \hline \ddot{x}_i \\ \ddot{x}_{i-1} \end{array}\right] = \left[\begin{array}{cc|cc} 0 & 1 & 0 & 0 \\ -\omega_f^2 & 0 & 1/m_i & 1/m_{i-1} \\ \hline -k_i/m_i & 0 & 1/m_i & 0 \\ k_i/m_{i-1} & 0 & 0 & -1/m_{i-1} \end{array}\right] \left[\begin{array}{c} \delta x_i \\ \dot{\delta x_i} \\ \hline f_{i+1/i} \\ f_{i/i-1} \end{array}\right].$$

This lower channel inversion can also be represented by the block-diagram depicted in Figure 11 where the lower channel of $Z_i(\mathbf{s})$ acts as a feedback on the inverse dynamic model of the mass m_{i-1}. One can recognize in this diagram the general approach presented in[2,9] to model a flexible appendage on a main body. The interest of this new approach is that the double port appendage model (here $Z_i(\mathbf{s})$) can be used to connect input port $f_{i+1/i}$ and output port $\ddot{x}_i$ to another appendage in series connection with $Z_i(\mathbf{s})$.

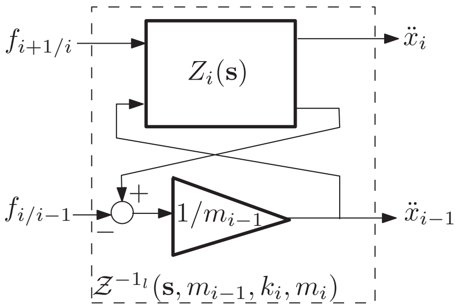

Figure 11. Block-diagram description of $\mathcal{Z}^{-1_l}(\mathbf{s}, m_{i-1}, k_i, m_i)$.

From the control design point of view, this last inversion is the most well-known: if we consider external forces applied on the spring-mass system, i.e.: $u_1 = f_{i+1/i}$ (child side) and $u_2 = -f_{i/i-1}$ (parent side), the transfer between accelerations (output) and forces (input) reads:

$$\left[\begin{array}{c} \ddot{x}_i \\ \ddot{x}_{i-1} \end{array}\right] = \underbrace{\frac{\left[\begin{array}{cc} m_{i-1}(\mathbf{s}^2+\omega_{c,c}^2) & m_i\omega_{c,p}^2 \\ m_{i-1}\omega_{c,c}^2 & m_i(\mathbf{s}^2+\omega_{c,p}^2) \end{array}\right]}{m_i m_{i-1}(\mathbf{s}^2+\omega_f^2)}}_{G(\mathbf{s})} \left[\begin{array}{c} u_1 \\ u_2 \end{array}\right]$$

where $\omega_{c,c} = \sqrt{\frac{k_i}{m_{i-1}}}$ is the "child cantilevered" frequency (that is, when the mass m_i is clamped on the inertial frame). One can recognize the free frequency ω_f in the denominator of $G(\mathbf{s})$, the "child cantilevered" frequency $\omega_{c,c}$ in the collocated upper left-hand transfer $(G(1,1))$ and the "parent cantilevered" frequency $\omega_{c,p}$ in the collocated lower right-hand transfer $(G(2,2))$.

These inversion operations on the double-port model allow to handle various constraints and boundary conditions. Indeed, these constraints and boundary conditions must be specified on the inputs of the subsystem model. It is thus now possible to specify that:

- the parent mass m_{i-1} of a subsystem i is free to move and submitted to an external force u using $\mathcal{Z}^{-1_l}(\mathbf{s}, m_{i-1}, k_i, m_i)$ and setting $f_{i/i-1} = -u$ ($\ddot{x}_{i-1}$ is now a free output),
- the child mass m_j of a subsystem j is locked using $\mathcal{Z}^{-1^u}(\mathbf{s}, m_{j-1}, k_j, m_j)$ and setting $\ddot{x}_j = 0$ ($f_{j+1/j}$ is now a free output and represents the lock force),
- if $j = i$ (m_{i-1} is free and submitted to an external force, m_i is locked) then $\mathcal{Z}^{-1}(\mathbf{s}, m_{i-1}, k_i, m_i)$ must be used to specify both boundary conditions on $\ddot{x}_i$ and $f_{i/i-1}$.

For instance, considering the actuated system depicted in Figure 12 and composed of 2 subsystems ($i = 1,\ 2$). The transfer between u and the 3 outputs $\ddot{x}_0$, $\ddot{x}_1$ and $f_{3/2}$ (the force locking m_2) can be described by the block diagram presented in Figure 13. The various boundary conditions for this example are summarized in Table 2.

i	$f_{i/i-1}$	$\ddot{x}_i$	$f_{i+1/i}$	$\ddot{x}_{i-1}$
1	$-u$	free	$f_{2/1}$	free
2	free	0	free	$\ddot{x}_1$

Table 2. Boundary conditions relative to the example depicted in Figure 12.

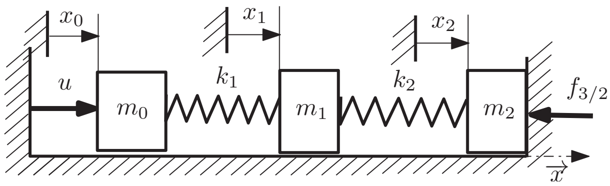

Figure 12. Another example.

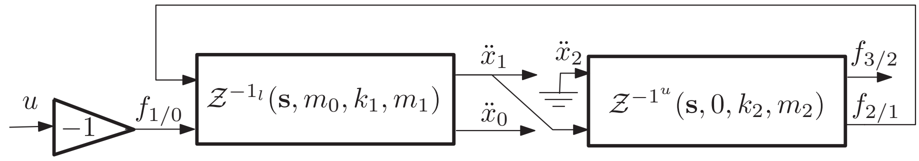

Figure 13. Block-diagram model of example depicted in Figure 12.

More generally, the following properties can easily be shown.
Properties:

- $\left[\mathcal{Z}^{-1_l}\right]^{-1} = \left[\mathcal{Z}^{-1}\right]^{-1_l} = \mathcal{Z}^{-1^u}$,
- $\left[\mathcal{Z}^{-1^u}\right]^{-1} = \left[\mathcal{Z}^{-1}\right]^{-1^u} = \mathcal{Z}^{-1_l}$,
- $\begin{bmatrix} 0 & -1 \\ 1 & 0 \end{bmatrix} \mathcal{Z}^{-1}(\mathbf{s}, m_{i-1}, k_i, m_i) \begin{bmatrix} 0 & -1 \\ 1 & 0 \end{bmatrix} = \mathcal{Z}(\mathbf{s}, m_i, k_i, m_{i-1})$.

III. Generalization

III.A. Objective

As shown in Figure 14, this section considers an intermediate flexible body (appendage or link) $\mathcal{A}$ linked to the parent structure $\mathcal{P}$ at the point P and to the child structure $\mathcal{C}$ at the point C. It is assumed that the only external forces and torques applied to $\mathcal{A}$ are the interactions with $\mathcal{P}$ and $\mathcal{C}$ at point P and C, respectively.

In the same spirit than the approach developped in the single-axis case, the objective is to build the double port model (12×12) of the body $\mathcal{A}$ such that:

$$\begin{bmatrix} \ddot{\mathrm{x}}_C \\ \mathrm{F}_{\mathcal{A}/\mathcal{P},P} \end{bmatrix} = M^{\mathcal{A}}_{P,C}(\mathbf{s}) \begin{bmatrix} \mathrm{F}_{\mathcal{C}/\mathcal{A},C} \\ \ddot{\mathrm{x}}_P \end{bmatrix} . \tag{8}$$

III.B. Principle

III.B.1. Clamped-free model

The modeling of the clamped (at point P) / free (at point C) body $\mathcal{A}$ using a finite-element approach is first considered (i.e.: $\mathrm{F}_{\mathcal{C}/\mathcal{A},C} = 0$). Let N_m the number of mesh nodes, considering the 3 translations and the 3 rotations of each nodes, the size of the vector q of the "flexible" degrees-of-freedom (d.o.f.) is $N = 6\,N_m$. Then, the finite element method:[3]

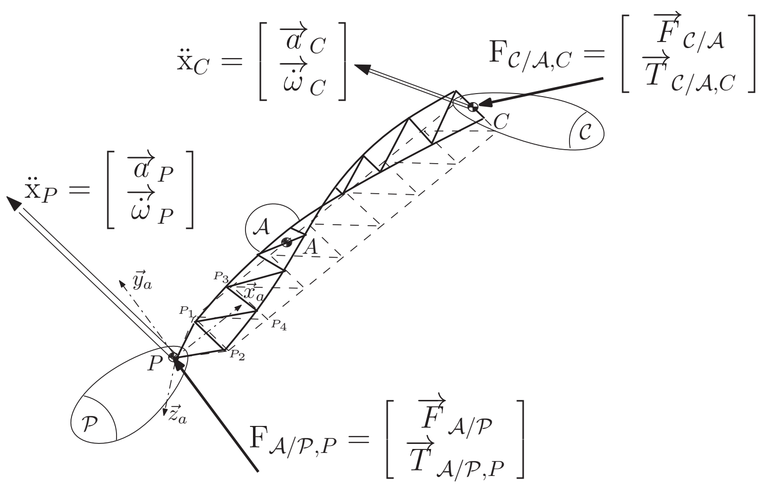

Figure 14. The intermediate body $\mathcal{A}$ in the structure.

- computes the dynamic model of the clamped-free body under the form of a the generalized 2nd-order differential equation:

$$\begin{bmatrix} M_{rr} & M_{rf} \\ M_{rf}^T & M_{ff} \end{bmatrix} \begin{bmatrix} \ddot{\mathrm{x}}_P \\ \ddot{q} \end{bmatrix} + \begin{bmatrix} 0_{6\times 6} & 0_{6\times N} \\ 0_{N\times 6} & K \end{bmatrix} \begin{bmatrix} \delta \mathrm{x}_P \\ q \end{bmatrix} = \begin{bmatrix} \mathrm{F}_{\mathcal{P}/\mathcal{A},P} \\ 0_{N\times 1} \end{bmatrix} = \begin{bmatrix} -\mathrm{F}_{\mathcal{A}/\mathcal{P},P} \\ 0_{N\times 1} \end{bmatrix} \tag{9}$$

  where $M_{rr} = D_P^{\mathcal{A}}$ is the direct dynamic model, at point P, of the body $\mathcal{A}$ assumed rigid:[2]

$$D_P^{\mathcal{A}} = \tau_{AP}^T \begin{bmatrix} m^{\mathcal{A}} I_3 & 0_{3\times 3} \\ 0_{3\times 3} & \mathbb{I}_A^{\mathcal{A}} \end{bmatrix} \tau_{AP} \ ,$$

  M_{ff}, M_{rf} are the mass submatrices associated to the flexible d.o.f. q and the rigid-flexible cross-coupling terms, respectively. K is the stifness matrix associated to the vector q.

- performs the modal analysis of the pair (M_{ff}, K), i.e.: computes the modal shape matrix Φ $(N \times N)$ and the flexible mode frequencies ω_i, $i = 1, \cdots, N$ such that:

$$(M_{ff}\omega_i^2 - K)\Phi(:, i) = 0, \quad \Phi^T M_{ff} \Phi = I_N, \quad \Phi^T K \Phi = \mathrm{diag}(\omega_i^2) \ .$$

The modal coordinate transformation $q = \Phi\eta$ in equation (9) leads to:

$$\begin{bmatrix} D_P^A & L_P^T \\ L_P & I_N \end{bmatrix} \begin{bmatrix} \ddot{\mathrm{x}}_P \\ \ddot{\eta} \end{bmatrix} + \begin{bmatrix} 0_{6\times 6} & 0_{6\times N} \\ 0_{N\times 6} & \mathrm{diag}(\omega_i^2) \end{bmatrix} \begin{bmatrix} \delta \mathrm{x}_P \\ \eta \end{bmatrix} = \begin{bmatrix} -\mathrm{F}_{\mathcal{A}/\mathcal{P},P} \\ 0_{N\times 1} \end{bmatrix} \ , \tag{10}$$

where $L_P = \Phi^T M_{rf}^T$ is the matrix $(N \times 6)$ of the modal participation factors. The i-th row of L_p, noted $l_{i,P}$, can be interpreted as the contribution of the i-th mode "acceleration" ($\ddot{\eta}_i$) to the force (3 components) and the torque (3 components) created inside the clamped joint located at point P, or by duality, how the i-th mode is "accelerated" due to an acceleration of the clamped joint located at point P.

A standard damping ratio ξ_i can then be taken into account on each modal coordinate. Then, equation (10) can be also expressed under:

- the hybrid-cantilever form:

$$-\mathrm{F}_{\mathcal{A}/\mathcal{P},P} = D_P^A \ddot{\mathrm{x}}_P + L_P^T \ddot{\eta}$$

$$\ddot{\eta} + diag(2\xi_i\omega_i)\dot{\eta} + diag(\omega_i^2)\eta = -L_P \ddot{\mathrm{x}}_P$$

- a state-space realization:

$$\begin{bmatrix} \dot{\eta} \\ \ddot{\eta} \end{bmatrix} = \begin{bmatrix} 0_{N\times N} & I_N \\ -\text{diag}(\omega_i^2) & -\text{diag}(2\xi_i\omega_i) \end{bmatrix} \begin{bmatrix} \eta \\ \dot{\eta} \end{bmatrix} + \begin{bmatrix} 0_{N\times 6} \\ -L_P \end{bmatrix} \ddot{\mathrm{x}}_P$$

$$\mathrm{F}_{\mathcal{A}/\mathcal{P},P} = \begin{bmatrix} L_P^T \,\text{diag}(\omega_i^2) & L_P^T \,\text{diag}(2\xi_i\omega_i) \end{bmatrix} \begin{bmatrix} \eta \\ \dot{\eta} \end{bmatrix} - \underbrace{(D_P^A - L_P^T L_P)}_{D_{P_0}^A} \ddot{\mathrm{x}}_P \,.$$

$D_{P_0}^A$ is the residual mass of $\mathcal{A}$ rigidly attached to $\mathcal{P}$ at point P.

- or the block diagram representation depicted in Figure 15 where the characteristic parameters ω_i, ξ_i, L_p and $D_{P_0}^A$ appear with a minimal occurence.

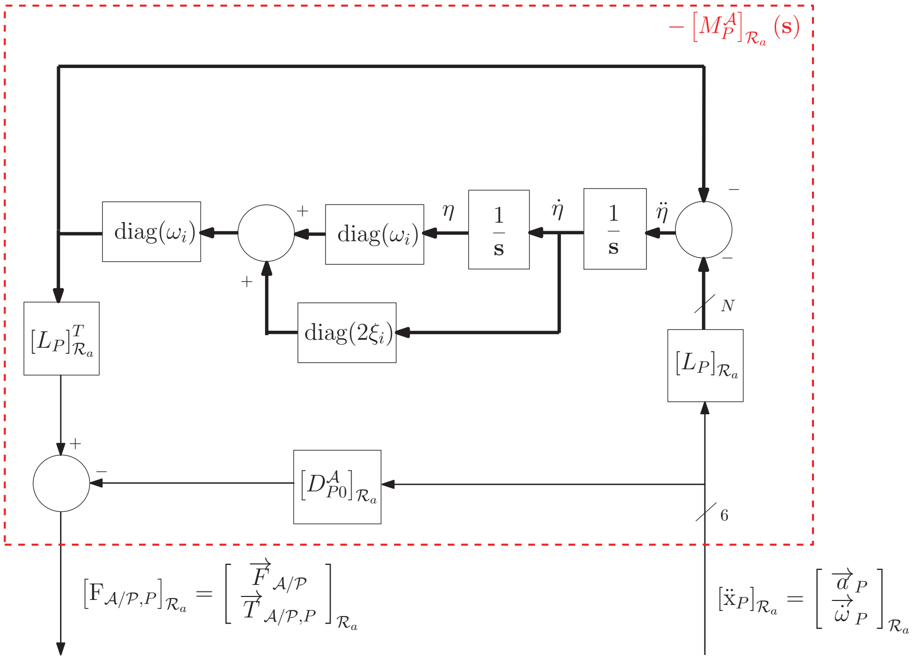

Figure 15. Block diagram representation of the cantilever-free model projected in the frame $\mathcal{R}_a$.

This is the model commonly used in space engineering to connect a flexible appendage on a rigd body (see also[2]). But in this model, the displacements of the various mesh nodes (particularly at the point C) are lost.

III.B.2. 2-port model

It is now assumed that:

- the meshing of $\mathcal{A}$ includes the point C,
- q is ordered such that the first 6 components correspond to the 6 displacements $\delta\mathrm{x}_C$ of the node C (w.r.t. the equilibrium position in $\mathcal{R}_a$).

The modal coordinate transformation $q = \Phi\eta$ can be written:

$$q = \begin{bmatrix} \delta\mathrm{x}_C \\ \delta\mathrm{x}_{\neq C} \end{bmatrix} = \begin{bmatrix} \Phi_C \\ \Phi_{\neq C} \end{bmatrix} \eta$$

where:

- $\delta \mathrm{x}_C$ is the (6×1) vector of the 6 displacements of the node C in $\mathcal{R}_a$,
- $\delta \mathrm{x}_{\neq C}$ is the $(6\,(N_m - 1) \times 1)$ vector of displacements at the other nodes $P_i \neq C$,
- Φ_C is the $(6 \times N)$ projection matrix of the N modal shapes on the 6 d.o.f $\delta \mathrm{x}_C$ ($\Phi_C = \Phi(1:6,:)$),
- $\Phi_{\neq C}$ is the $((N-6) \times N)$ projection matrix of the N modal shapes on the other d.o.f.

Under the linearity assumption (the second order terms are neglected in the composition of accelerations), it is now possible to express the acceleration at point C considering the 2 contributions:

- the acceleration due to the deformation of $\mathcal{A}$: $\Phi_C \ddot{\eta}$ (to be projected in $\mathcal{R}_a$),
- the acceleration due to "whole" acceleration of $\mathcal{A}$ at point P, translated to C through the kinematic model τ_{CP}: $\tau_{CP}\ddot{\mathrm{x}}_P$ (to be projected in $\mathcal{R}_a$):

$$\boxed{\ddot{\mathrm{x}}_c = \tau_{CP}\ddot{\mathrm{x}}_P + \Phi_C\ddot{\eta} = [\tau_{CP} \quad \Phi_C] \begin{bmatrix} \ddot{\mathrm{x}}_P \\ \ddot{\eta} \end{bmatrix}.} \tag{11}$$

It is also possible to take into account that the body $\mathcal{A}$ is submitted to an external force $\mathrm{F}_{\mathcal{C}/\mathcal{A},C}$ at point C, thanks to virtual work principle. The left-hand term of model (9) must be completed by the generalized force due to the work of $\mathrm{F}_{\mathcal{C}/\mathcal{A},C}$ which reads:

$$\mathcal{W}(\mathrm{F}_{\mathcal{C}/\mathcal{A},C}) = (\tau_{CP}\delta\mathrm{x}_P + \delta\mathrm{x}_C)^T \mathrm{F}_{\mathcal{C}/\mathcal{A},C} = \begin{bmatrix} \delta\mathrm{x}_P \\ \eta \end{bmatrix}^T [\tau_{CP} \quad \Phi_C]^T \,\mathrm{F}_{\mathcal{C}/\mathcal{A},C}\,.$$

Then model (9) becomes:

$$\begin{bmatrix} M_{rr} & M_{rf} \\ M_{rf}^T & M_{ff} \end{bmatrix} \begin{bmatrix} \ddot{\mathrm{x}}_P \\ \ddot{q} \end{bmatrix} + \begin{bmatrix} 0_{6\times6} & 0_{6\times N} \\ 0_{N\times6} & K \end{bmatrix} \begin{bmatrix} \delta\mathrm{x}_P \\ q \end{bmatrix} = \begin{bmatrix} -\mathrm{F}_{\mathcal{A}/\mathcal{P},P} + \tau_{CP}^T \mathrm{F}_{\mathcal{C}/\mathcal{A},C} \\ \begin{bmatrix} \mathrm{F}_{\mathcal{C}/\mathcal{A},C} \\ 0_{(N-6)\times1} \end{bmatrix} \end{bmatrix} \tag{12}$$

and, through the modal coordinate transformation, model (10) reads:

$$\boxed{\begin{bmatrix} D_P^A & L_P^T \\ L_P & I_N \end{bmatrix} \begin{bmatrix} \ddot{\mathrm{x}}_P \\ \ddot{\eta} \end{bmatrix} + \begin{bmatrix} 0_{6\times6} & 0_{6\times N} \\ 0_{N\times6} & \mathrm{diag}(\omega_i^2) \end{bmatrix} \begin{bmatrix} \delta\mathrm{x}_P \\ \eta \end{bmatrix} = \begin{bmatrix} -\mathrm{F}_{\mathcal{A}/\mathcal{P},P} + \tau_{CP}^T \mathrm{F}_{\mathcal{C}/\mathcal{A},C} \\ \Phi_C^T \mathrm{F}_{\mathcal{C}/\mathcal{A},C} \end{bmatrix}.} \tag{13}$$

From equations (11) and (13), the double port model $M_{PC}^{\mathcal{A}}(\mathbf{s})$ of the body $\mathcal{A}$ defined in equation (8) can be expressed (modal damping ratios are now considered):

- by the **extented** hybrid cantilever form:

$$-\mathrm{F}_{\mathcal{A}/\mathcal{P},P} = D_P^A \ddot{\mathrm{x}}_P + L_P^T \ddot{\eta} - \tau_{CP}^T \mathrm{F}_{\mathcal{C}/\mathcal{A},C}$$

$$\ddot{\eta} + diag(2\xi_i\omega_i)\dot{\eta} + diag(\omega_i^2)\eta = -L_P \ddot{\mathrm{x}}_P + \Phi_C^T \mathrm{F}_{\mathcal{C}/\mathcal{A},C}\ ,$$

- by the state-space realization:

$$\boxed{\begin{bmatrix} \dot{\eta} \\ \ddot{\eta} \\ \hline \ddot{\mathrm{x}}_C \\ \mathrm{F}_{\mathcal{A}/\mathcal{P},P} \end{bmatrix} = \left[\begin{array}{cc|cc} 0_{N\times N} & I_N & 0_{N\times6} & 0_{N\times6} \\ -\mathrm{diag}(\omega_i^2) & -\mathrm{diag}(2\xi_i\omega_i) & \Phi_C^T & -L_P \\ \hline -\Phi_C\,\mathrm{diag}(\omega_i^2) & -\Phi_C\,\mathrm{diag}(2\xi_i\omega_i) & \Phi_C\Phi_C^T & (\tau_{CP} - \Phi_C\,L_P) \\ L_P^T\,\mathrm{diag}(\omega_i^2) & L_P^T\,\mathrm{diag}(2\xi_i\omega_i) & (\tau_{CP} - \Phi_C\,L_P)^T & -D_{P_0}^A \end{array}\right] \begin{bmatrix} \eta \\ \dot{\eta} \\ \hline \mathrm{F}_{\mathcal{C}/\mathcal{A},C} \\ \ddot{\mathrm{x}}_P \end{bmatrix}} \tag{14}$$

  where $D_{P_0}^A = D_P^A - L_p^T L_P$.

- by the block diagram representation depicted in Figure 16 where the characteristic parameters ω_i, ξ_i, L_p, $D_{P_0}^A$, Φ_C and τ_{CP} appear with a minimal occurence. These parameters can be provided by finite element softwares.

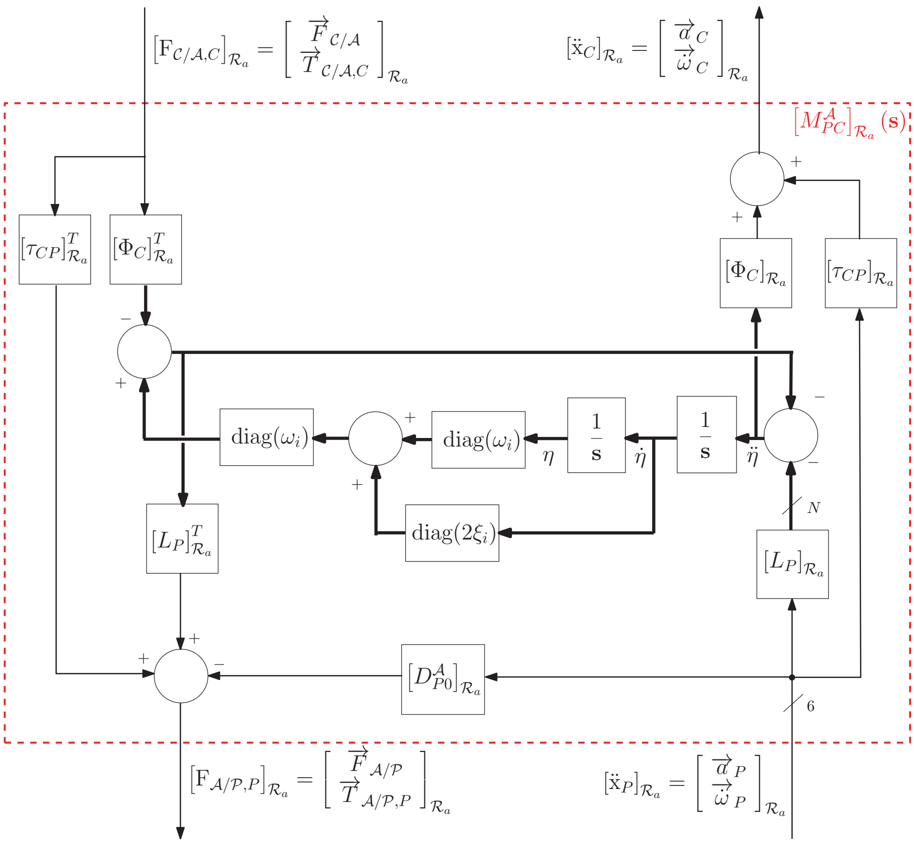

Figure 16. Block diagram representation of the two-port model $M^{\mathcal{A}}_{PC}(\mathbf{s})$ projected in the frame $\mathcal{R}_a$.

- by a port-hamiltonian representation. Equation (12), taking into account the damping matrix D, and equation (11) can be rewriten:

$$\begin{bmatrix} M_{rr} & M_{rf} \\ M_{rf}^T & M_{ff} \end{bmatrix} \begin{bmatrix} \ddot{\mathrm{x}}_P \\ \ddot{q} \end{bmatrix} + \begin{bmatrix} 0_{6\times 6} & 0_{6\times N} \\ 0_{N\times 6} & D \end{bmatrix} \begin{bmatrix} * \\ \dot{q} \end{bmatrix} + \begin{bmatrix} 0_{6\times 6} & 0_{6\times N} \\ 0_{N\times 6} & K \end{bmatrix} \begin{bmatrix} * \\ q \end{bmatrix} = \begin{bmatrix} -\mathrm{F}_{\mathcal{A}/\mathcal{P},P} + \tau_{CP}^T \mathrm{F}_{\mathcal{C}/\mathcal{A},C} \\ S^T \mathrm{F}_{\mathcal{C}/\mathcal{A},C} \end{bmatrix} \tag{15}$$

and

$$\ddot{\mathrm{x}}_C = \tau_{CP}\ddot{\mathrm{x}}_P + S\ddot{q}\,. \tag{16}$$

where S is a $N \times 6$ selection matrix (with 0 or 1 elements) of the 6 d.o.fs of the meshing node where is applied $\mathrm{F}_{\mathcal{C}/\mathcal{A},C}$ ($S = \Phi_C\,\Phi^{-1}$). Then, the port-hamiltonian representation reads:

$$\boxed{\begin{array}{l} \left\{\begin{array}{rcl} \dot{q} & = & \frac{\partial H}{\partial p} \\ \dot{p} & = & -\frac{\partial H}{\partial q} - D\dot{q} + \begin{bmatrix} S^T & -M_{rf}^T \end{bmatrix} \begin{bmatrix} \mathrm{F}_{\mathcal{C}/\mathcal{A},C} \\ \ddot{\mathrm{x}}_P \end{bmatrix} \end{array}\right. \\ \begin{bmatrix} \ddot{\mathrm{x}}_C \\ \mathrm{F}_{\mathcal{A}/\mathcal{P},P} \end{bmatrix} = \begin{bmatrix} S \\ -M_{rf} \end{bmatrix} M_{ff}^{-1}\,\dot{p} + \begin{bmatrix} 0 & \tau_{CP} \\ \tau_{CP}^T & -M_{rr} \end{bmatrix} \begin{bmatrix} \mathrm{F}_{\mathcal{C}/\mathcal{A},C} \\ \ddot{\mathrm{x}}_P \end{bmatrix} \end{array}} \tag{17}$$

where $H = \frac{1}{2}p^T M_{ff}^{-1} p + \frac{1}{2}q^T K q$ and $p = M_{ff}\dot{q}$.

In the notation $M_{PC}^{\mathcal{A}}(\mathbf{s})$:

- P (the first indice) stands for the clamped point used to build the model. The lower channel is the 6×6 direct dynamic model of $\mathcal{A}$ at point P,
- C (the second indice) stands for the free point which can be loaded by a child substructure. The upper channel is the 6×6 inverse dynamic model of $\mathcal{A}$ at point C.

By setting its inputs to 0, $M_{PC}^{\mathcal{A}}(\mathbf{s})$ represents the clamped (at P) - free (at C) model of $\mathcal{A}$. In the same way, $\left[M_{PC}^{\mathcal{A}}\right]^{-1}(\mathbf{s})$ represents the free (at P) - clamped (at C) model of $\mathcal{A}$.

Both channels are invertible. Exactly as in the single-axis case, the inverse models:

- $\left[M_{PC}^{\mathcal{A}}\right]^{-1^u}(\mathbf{s})$ such that:

$$\begin{bmatrix} \mathrm{F}_{\mathcal{C}/\mathcal{A},C} \\ \mathrm{F}_{\mathcal{A}/\mathcal{P},P} \end{bmatrix} = \left[M_{PC}^{\mathcal{A}}\right]^{-1^u}(\mathbf{s}) \begin{bmatrix} \ddot{\mathrm{x}}_C \\ \ddot{\mathrm{x}}_P \end{bmatrix},$$

- $\left[M_{PC}^{\mathcal{A}}\right]^{-1_l}(\mathbf{s})$ such that:

$$\begin{bmatrix} \ddot{\mathrm{x}}_C \\ \ddot{\mathrm{x}}_P \end{bmatrix} = \left[M_{PC}^{\mathcal{A}}\right]^{-1_l}(\mathbf{s}) \begin{bmatrix} \mathrm{F}_{\mathcal{C}/\mathcal{A},C} \\ \mathrm{F}_{\mathcal{A}/\mathcal{P},P} \end{bmatrix},$$

can be used to take into account boundary conditions. $\left[M_{PC}^{\mathcal{A}}\right]^{-1^u}(\mathbf{s})$ represents the clamped (at P) - clamped (at C) model of $\mathcal{A}$ and $\left[M_{PC}^{\mathcal{A}}\right]^{-1_l}(\mathbf{s})$ represents the free (at P) - free (at C) model of $\mathcal{A}$.

It is also possible to take into account a second (or more) child substructure(s) $\mathcal{C}'$ connected to $\mathcal{A}$ at point C' by augmenting the model by another 6×6 upper channel. The model $M_{PCC'}^{\mathcal{A}}(\mathbf{s})$ is then associated to the following state-space realization:

$$\left[\begin{array}{c} \dot{\eta} \\ \ddot{\eta} \\ \hline \ddot{\mathrm{x}}_{C'} \\ \ddot{\mathrm{x}}_C \\ \mathrm{F}_{\mathcal{A}/\mathcal{P},P} \end{array}\right] = \left[\begin{array}{cc|ccc} 0_{N\times N} & I_N & 0_{N\times 6} & 0_{N\times 6} & 0_{N\times 6} \\ -\mathrm{diag}(\omega_i^2) & -\mathrm{diag}(2\xi_i\omega_i) & \Phi_{C'}^T & \Phi_C^T & -L_P \\ \hline -\Phi_{C'}\,\mathrm{diag}(\omega_i^2) & -\Phi_{C'}\,\mathrm{diag}(2\xi_i\omega_i) & \Phi_{C'}\Phi_{C'}^T & \Phi_{C'}\Phi_C^T & (\tau_{C'P} - \Phi_{C'}\,L_P) \\ -\Phi_C\,\mathrm{diag}(\omega_i^2) & -\Phi_C\,\mathrm{diag}(2\xi_i\omega_i) & \Phi_C\Phi_{C'}^T & \Phi_C\Phi_C^T & (\tau_{CP} - \Phi_C\,L_P) \\ L_P^T\,\mathrm{diag}(\omega_i^2) & L_P^T\,\mathrm{diag}(2\xi_i\omega_i) & (\tau_{C'P} - \Phi_{C'}\,L_P)^T & (\tau_{CP} - \Phi_C\,L_P)^T & -D_{P_0}^{A} \end{array}\right] \left[\begin{array}{c} \eta \\ \dot{\eta} \\ \hline \mathrm{F}_{\mathcal{C}'/\mathcal{A},C'} \\ \mathrm{F}_{\mathcal{C}/\mathcal{A},C} \\ \ddot{\mathrm{x}}_P \end{array}\right].$$

For instance the structure depicted in Figure 17 is composed of a main body $\mathcal{B}$ and two appendages $\mathcal{A}_1$ and $\mathcal{A}_2$, connected to $\mathcal{B}$ in points C_1 and C_2, respectively. The body $\mathcal{B}$ is submitted to an external force (dual) vector U at point P. The transfer, from U (6 inputs) to the acceleration dual vector $\ddot{\mathrm{x}}_P$ at point P of $\mathcal{B}$ and the 2 acceleration dual vectors $\ddot{\mathrm{x}}_{F_1}$ and $\ddot{\mathrm{x}}_{F_2}$ at ending points F_1 and F_2 of $\mathcal{A}_1$ and $\mathcal{A}_2$ (18 outputs),

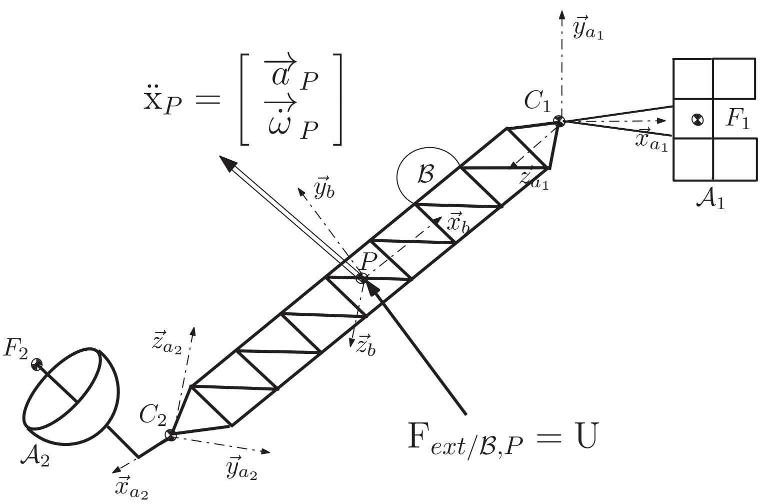

Figure 17. A system with 3 flexible bodies.

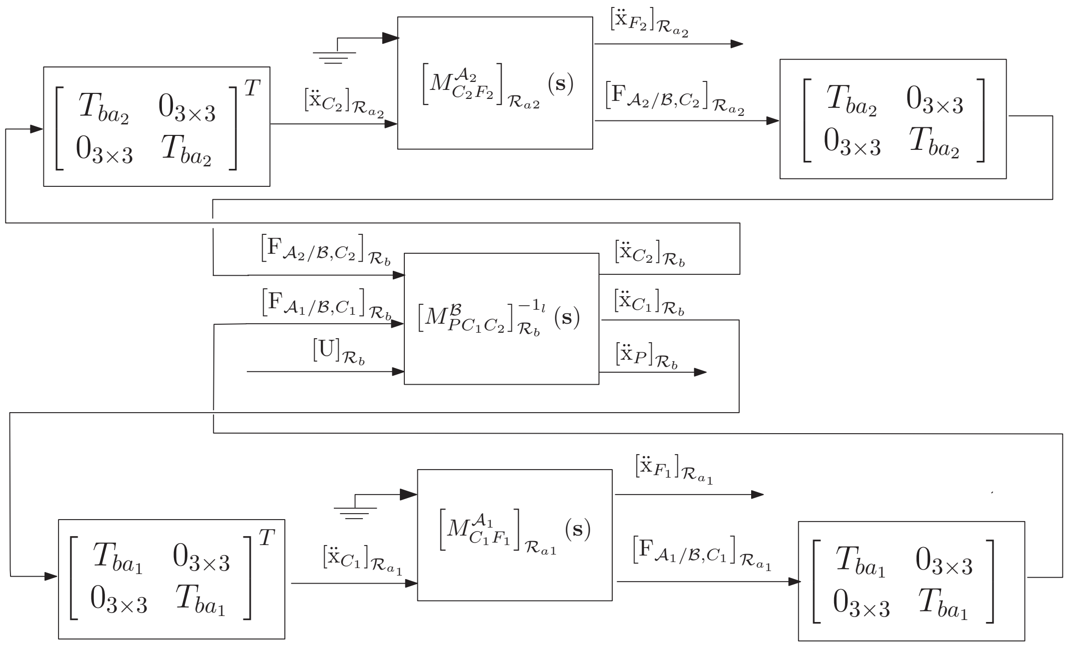

Figure 18. The block-diagram model of example depicted in Figure 17.

can be represented by the block-diagram of Figure 18 where T_{ba_i} $(i = 1, 2)$ is the direction cosine matrix between frames $\mathcal{R}_b$ and $\mathcal{R}_{a_i}$ (i.e.: the matrix of components of unitary vectors $\vec{x}_{a_i}$, $\vec{y}_{a_i}$, $\vec{z}_{a_i}$ in $\mathcal{R}_b$).

In comparison with the approach presented in,[2,9] this new approach allows the modeling of open-chain of flexible bodies. Note that the possibility, presented in,[2] to take into account a revolute joint at the connection point P between bodies $\mathcal{A}$ and $\mathcal{P}$ (see Figure 19) is still possible.

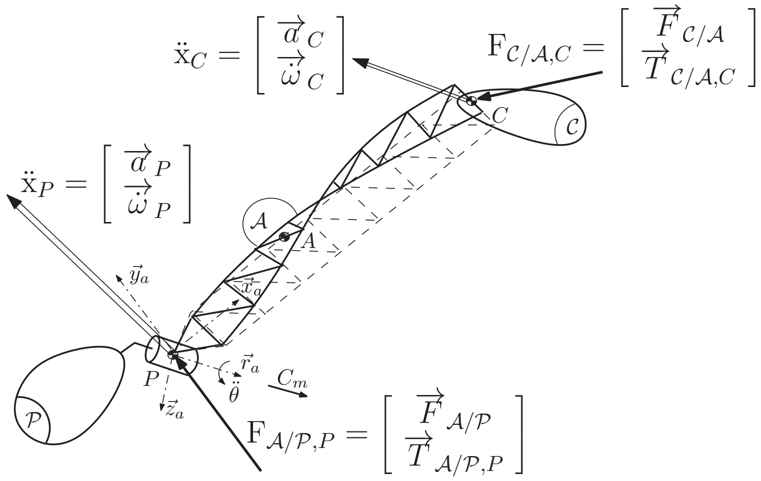

Figure 19. Appendage $\mathcal{A}$ in connection with $\mathcal{P}$ through a revolute joint along $\vec{r}_a$.

Indeed, one can express the augmented (13×13) double port model $\left[G^{\mathcal{A}}_{PC}\right]_{\mathcal{R}_a}(\mathbf{s})$ of the body $\mathcal{A}$ projected in the frame $\mathcal{R}_a$: let $\vec{r}_a = \begin{bmatrix} x_{r_a} \\ y_{r_a} \\ z_{r_a} \end{bmatrix}_{\mathcal{R}_a}$ be a unit vector along the revolute joint axis, then:

$$\begin{bmatrix} \begin{bmatrix} \ddot{\mathrm{x}}_C \\ \mathrm{F}_{\mathcal{A}/\mathcal{P},P} \end{bmatrix}_{\mathcal{R}_a} \\ C_m \end{bmatrix} = \underbrace{\begin{bmatrix} & I_{12} & \\ \underbrace{0 \cdots 0}_{\times 9} & x_{r_a} \; y_{r_a} \; z_{r_a} \end{bmatrix} \left[M^{\mathcal{A}}_{P,C}\right]_{\mathcal{R}_a}(\mathbf{s}) \begin{bmatrix} & \left.\begin{matrix} 0 \\ \vdots \\ 0 \end{matrix}\right\} \times 9 \\ I_{12} & \\ & x_{r_a} \\ & y_{r_a} \\ & z_{r_a} \end{bmatrix}}_{\left[G^{\mathcal{A}}_{PC}\right]_{\mathcal{R}_a}(\mathbf{s})} \begin{bmatrix} \begin{bmatrix} \mathrm{F}_{\mathcal{C}/\mathcal{A},C} \\ \ddot{\mathrm{x}}_P \end{bmatrix}_{\mathcal{R}_a} \\ \ddot{\theta} \end{bmatrix}. \tag{18}$$

$\left[G^{\mathcal{A}}_{PC}\right]_{\mathcal{R}_a}(\mathbf{s})$ is the 2-port model augmented with a 13th input: $\ddot{\theta}$, the angular acceleration inside the revolute joint and a 13th output: C_m the torque applied by an actuator located inside the revolute joint.

That's make possible to free some degrees-of-freedom (setting $C_m = 0$) or to take into account the model $K(s)$ of a local mechanism (gear-box, ...) inside an actuated revolute joint (for instance, for space robotic arm modelling) according to Figure 20. In this case, one will have to inverse the system $\left[G^{\mathcal{A}}_{PC}\right]_{\mathcal{R}_a}(\mathbf{s})$ between its 13-th input and its 13-th output and one can define a new inversion operation: let $\left[G^{\mathcal{A}}_{PC}\right]^{-1_p}_{\mathcal{R}_a}(\mathbf{s})$ be the operation corresponding to the inversion of the 13-th input output channel of $\left[G^{\mathcal{A}}_{PC}\right]_{\mathcal{R}_a}(\mathbf{s})$ such that:

$$\begin{bmatrix} \begin{bmatrix} \ddot{\mathrm{x}}_C \\ \mathrm{F}_{\mathcal{A}/\mathcal{P},P} \end{bmatrix}_{\mathcal{R}_a} \\ \ddot{\theta} \end{bmatrix} = \left[G^{\mathcal{A}}_{PC}\right]^{-1_p}_{\mathcal{R}_a}(\mathbf{s}) \begin{bmatrix} \begin{bmatrix} \mathrm{F}_{\mathcal{C}/\mathcal{A},C} \\ \ddot{\mathrm{x}}_P \end{bmatrix}_{\mathcal{R}_a} \\ C_m \end{bmatrix}.$$

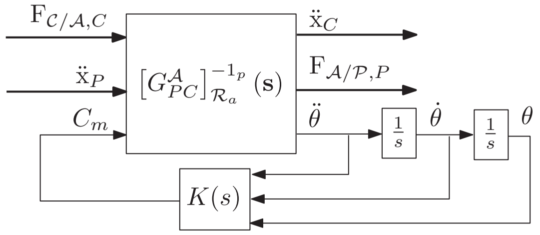

Figure 20. Taking into account a local mechanism model $K(s)$ in the 2-port model of a body $\mathcal{A}$.

IV. Conclusions and Perspectives

The main contribution of this work is to proposed a general formalism to model mechanical systems composed of various sub-systems with lumped boundary conditions. This formalism is linked to port-Hamiltonian systems in the sense that the 2-port model of each substructures can be described by a port-Hamiltonian model but mainly in the sense that the definition of the inputs and the outputs of the sub-system are completely revisited and not a priori defined. The 2-port model considers transfer linking forces and accelerations in both senses. The main property of the 2-port model is that it can be inverted channel by channel. It was also shown that finite element methods can be used to provide a 2-port model, easily implementable under common MATLAB® working environment. The approacch can be used to build a structured dynamic model of complex mechanical system where the parameters of local mechanisms between substructures can be easily isolated in order to be optimized in a co-design procedure.

Some further works are still required to:

- extend and validate the proposed approach to mechanical system with closed kinematic chains,
- extend the approach to handle distributed boundary conditions.

Considering a lumped approximation of the distributed boundary conditions, these 2 extensions are linked and one of the objective must be to develop practical tools to handle infinite-dimension port-Hamiltonian systems with not a so huge finite-dimension numerical models.

Acknowledgements

The authors would like to thank CHRISTELLE PITTET from CNES, FINN ANKERSEN from ESA and CHIARA TOGLIA from Thales Alenia Space Italy for their supports.

References

[1]Alazard, D., Loquen, T., de Plinval, H., and and, C. C., "Avionics/Control co-design for large flexible space structures." *AIAA Guidance Navigation and Control conference*, Boston (Massachusetts), August 2013.

[2]Alazard, D., Cumer, C., and Tantawi, K., "Linear dynamic modeling of spacecraft with various flexible appendages and on-board angular momentums," *Proceeding of the 7^{th} International ESA Conference on Guidance, Navigation and Control Systems*, Tralee (Ireland), June 2008.

[3]Craig, R. and Bampton, M., "Coupling of substructures for dynamic analyses." *AIAA Journal*, Vol. 6 (7), July 1968.

[4]Rixen, D. J., "A dual Craig-Bampton method for dynamic substructuring," *Journal of Computational and Applied Mathematics*, Vol. 168, No. 1-2, 2004, pp. 383 – 391.

[5]Ramirez, H., Zwarrt, H., and Gorrec, Y. L., "Exponential stability of boundary controlled port Hamiltonian systems with dynamic feedback." *1st IFAC Workshop on Control of Systems Governed by Partial Differential Equations*, Paris (France), Setpember 2013.

[6]Ortega, R., van der Schaft, A., Maschke, B., and Escobar, G., "Interconnection and damping assignment passivity-based control of port-controlled Hamiltonian systems." *Automatica*, Vol. 38 (4), 2002, pp. 585–596.

[7]Matignon, D. and Hélie, T., "A class of damping models preserving eigenspaces for linear conservative port-Hamiltonian systems." *European Journal of control*, Vol. 19 (6), 2013, pp. 486–494.

[8]Guy, N., Alazard, D., Cumer, C., and Charbonnel, C., "Dynamic modeling and analysis of spacecraft with variable tilt of flexible appendages," *ASME - Journal of Dynamic Systems Measurement and Control*, Vol. 136 (2), January 2014.

[9]Loquen, T., de Plinval, H., Cumer, C., and Alazard, D., "Attitude control of satellites with flexible appendages: a structured H_∞ control design." *AIAA Guidance Navigation and Control conference*, Mineapolis (Minnesota), August 2012.